

Fused Deposition Modeling 3D Printing-based Flexible Bending Sensor

Sun Kon Lee*, Young Chan Oh*, Joo Hyung Kim*[#]

*Department of Mechanical Engineering, Inha University

FDM 3D프린팅 기반 유연굽힘센서

이선곤*, 오영찬*, 김주형*[#]

*인하대학교 기계공학과

(Received 21 October 2019; received in revised form 14 November 2019; accepted 24 November 2019)

ABSTRACT

Recently, to improve convenience, flexible electronics are quickly being developed for a number of application areas. Flexible electronic devices comprise characters such as being bendable, stretchable, foldable, and wearable. Effectively manufacturing flexible electronic devices requires high efficiency, low costs, and simple processes for manufacturing technology. Through this study, we enabled the rapid production of multifunctional flexible bending sensors using a simple, low-cost Fused Deposition Modeling (FDM) 3D printer. Furthermore, we demonstrated the possibility of the rapid production of a range of functional flexible bending sensors using a simple, low-cost FDM 3D printer. Accurate and reproducible functional materials made by FDM 3D printers are an effective tool for the fabrication of flexible sensor electronic devices. The 3D-printed flexible bending sensor consisted of polyurethane and a conductive filament. Two patterns of electrodes (straight and Hilbert curve) for the 3D printing flexible sensor were fabricated and analyzed for the characteristics of bending displacement. The experimental results showed that the straight curve electrode sensor sensing ability was superior to the Hilbert curve electrode sensor, and the electrical conductivity of the Hilbert curve electrode sensor is better than the straight curve electrode sensor. The results of this study will be very useful for the fabrication of various 3D-printed flexible sensor devices with multiple degrees of freedom that are not limited by size and shape.

Key Words : Additive Manufacturing(적층가공), Conductive 3D Printing(전도성 3D프린팅), 3D Printing Annealing(3D 프린팅 어닐링) 3D Printing Flexible Bending Sensor(3D프린팅 유연굽힘센서), Flexible Electronic Devices(유연 전자 디바이스)

1. Introduction

In recent years, many studies have been conducted

on flexible electronic devices (FEDs), yielding many developments that improve quality of life and convenience in many areas, such as wearables, displays, haptic, entertainment, and rehabilitation to name a few. FEDs should be able to be bendable, stretchable, rollable, foldable, and ultimately wearable.

[#] Corresponding Author : sun@inha.ac.kr

Tel: +82-32-860-7320, Fax: +82-32-868-6430

Fig. 1 shows the photo-lithograph process, which is widely used in current flexible sensor production. This production process is complex and requires expensive materials and equipment for each use^[1]. It has also drawbacks such as high degree of freedom (DOF) implementation and limitations on shape and size. Thus, much attention has been paid to developing various printing-based flexible sensor production techniques with simple and low-cost production.

Fig. 2 shows the flexible sensor printing processes that are currently widely used such as ink jet, nozzle, screen, and roll-to-roll^[2-6]. The ink jet printing sprays ink to the flexible substrate and produce a device. The nozzle printing is utilized to produce a line or plane pattern. The screen process without using a nozzle makes it relatively easy to select materials and can produce a thick pattern. The roll-to-roll process produces a pattern by passing a flexible substrate between rolls, which makes it easy to control thickness. However, these printing processes have the following drawbacks: complex processes that are not yet familiar to the public, high production cost, and limitation of size and shape. Thus, this study aims to produce an FED with a simple process and low production cost using a fused deposition modeling (FDM) three-dimensional (3D) printer, which is widely distributed to the public, and analyze its characteristics.

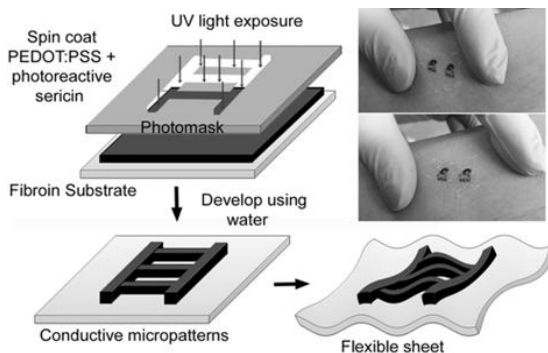


Fig. 1 Schematic of PhotoLithograph process^[1]

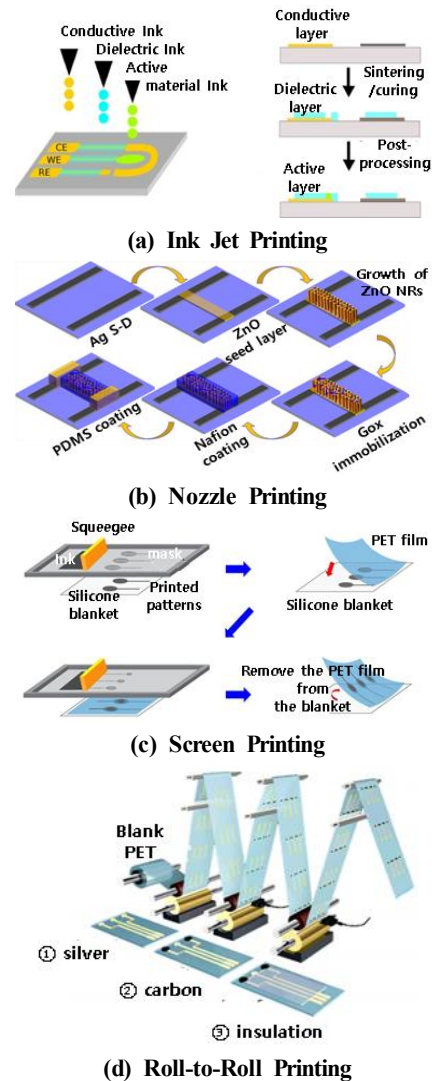


Fig. 2 Schematic of printing sensor process^[2-6]

This study produces a flexible bending sensor (FBS) that can be produced easily and facilitate intuitive judgment, using FDM 3D printing, and its performance is discussed. This will contribute to the promotion of FDM 3D printing use, departing from the simple structure production by expanding the utilization field of FDM 3D printing into various application areas including electronics and controls.

2. Experiment and discussion

To evaluate the characteristics of electrical resistance according to the bending displacement of the FDM 3D printing FBS, an FBS was manufactured using 3D printing of straight and Hilbert curve electrodes inside thermoplastic polyurethane (TPU) as shown in Fig. 3. To compare the performance between straight and Hilbert curve electrode sensors, the electrode surface area was designed equivalently to have 1125 mm^2 .

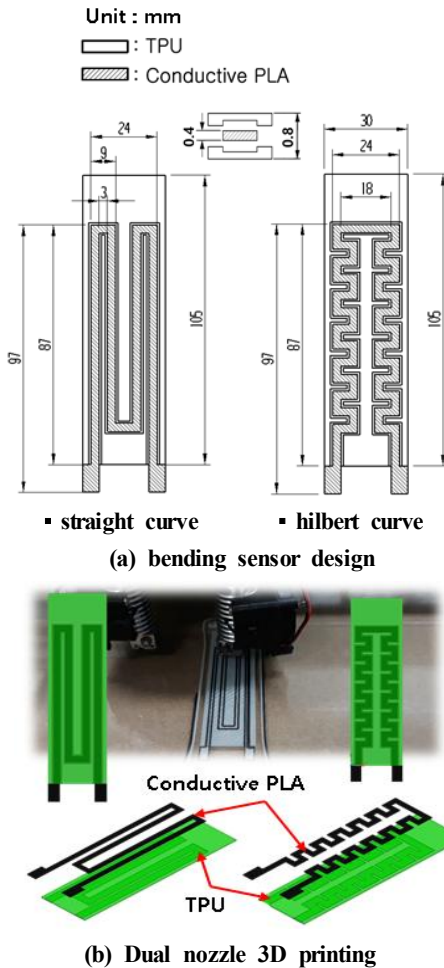


Fig. 3 Design and Fabrication of 3D printing flexible bending sensor

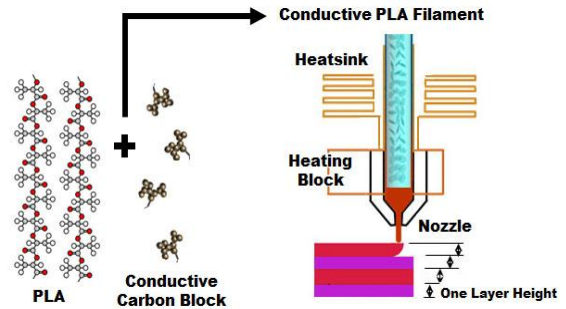


Fig. 4 Simplified schematics depicting the process of conductive PLA-based 3D printing using the technique of FDM^[7].

The principle of 3D printing FBS is to measure bending displacement of the sensor using the electric resistance characteristics of thin plate electrode printed with conductive filaments. The conductive filaments used in the 3D printing electrode are a composite of conductive carbon black and Natureworks 4043D polylactic acid (PLA), with 15 wt. % of carbon black. The conceptual diagram of the conductive filament 3D printing is shown in Fig. 4.

Fig. 5 shows the 3D printing process of FBS, in which TPU is layered and, for electrode printing and electrode supporting, TPU is re-layered to have a structure of inserted electrode inside the TPU. The 3D printing electrode has a brittleness characteristic. Thus, the electrode support was composed of flexible TPU to support the bending displacement of the electrode.

The characteristic of the 3D printing FBS was evaluated by measuring the change in electric resistance according to displacement while applying 10-, 20-, and 30-mm bending displacement at a 1-mm/sec rate in the sensor's center in real time using a digital multi-meter (34410a, Agilent) as shown in Fig. 6. In addition, the change in electrical characteristics was measured using the same method after annealing of 3D printing FBS in a constant temperature oven, allowing comparative analysis of the

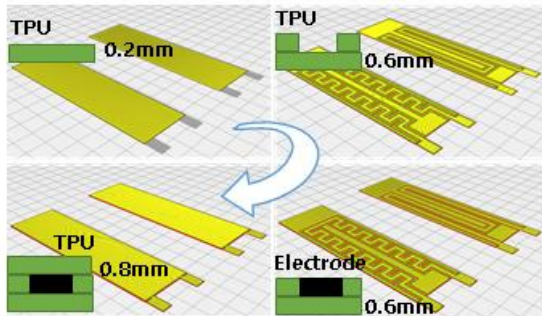


Fig. 5 Simplified depicting the process of 3D printing bending sensor

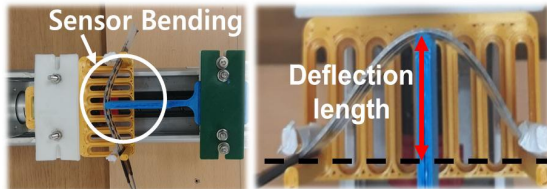


Fig. 6 3D printing Flexible bending sensor characteristic evaluation system. (1-axial PLC actuator)

characteristics before and after annealing.

The glass transition temperature (T_g) and crystallization temperature of the conductive PLA filament, which was used as an electrode of the bending sensor, were measured using a differential scanning calorimeter (DSC) to determine the appropriate temperature for annealing of the FBS. The measurement results were: PLA and carbon block's T_g were approximately 62°C and 880 °C, respectively, and the PLA crystallization temperature was approximately 120°C. Thus, the annealing temperature was set to 120°C. The measurement equipment used was DSC200F3 manufactured by NETZSCH^[7-8].

2.1 Electrical characteristic test of 3D printing FBS

To evaluate the characteristics according to the

displacement of 3D printing FBS, the change in electric resistance was measured in real time while applying 10, 20, and 30% increase in bending displacement followed by 5-sec. stay and returning-back using a programmable logic controller (PLC), which was conducted five times, respectively, after fixing the bending sensor at the single-axis actuator.

Fig. 7 shows the change in electric resistance against iterative bending displacement. Fig. 7(a) shows the curve of the change in electric resistance against 10-mm bending displacement in the bending sensor center, in which the electric resistance value increased in proportional to the increase in displacement over time, as presented in Eq. (1).

The measurement results of electric resistance in straight and Hilbert curve electrode sensors showed that the electric resistance value of the Hilbert curve electrode sensor was lower even in the same electrode surface area (1125mm²) and displacement. This was because of the increase in displacement of the electrode due to the difference in electrode design and a relatively shorter travel distance of the high-temperature nozzle during the Hilbert curve electrode printing lamination, thereby having less occurrence of residual stress caused by high-temperature extrusion and cooling of the printing nozzle. The electric resistance changes (ΔR = maximum resistance - initial resistance) of the straight and Hilbert curve electrode sensors were 0.3k Ω and 0.13k Ω , respectively.

Fig. 7(b) and (c) show the electric resistance curves against 20- and 30-mm bending displacements in the bending sensor center, in which the electric resistance increases proportionally to the increase in bending displacement.

The electric resistance change (ΔR) against 20- and 30-mm bending displacement in the bending sensor center was 0.82 and 1.45 k Ω in the straight curve sensor, and 0.42 and 1.03 k Ω in the Hilbert curve sensor, which also showed that the electric

resistance change of the Hilbert curve electrode sensor was smaller, as in the case of 10-mm bending displacement.

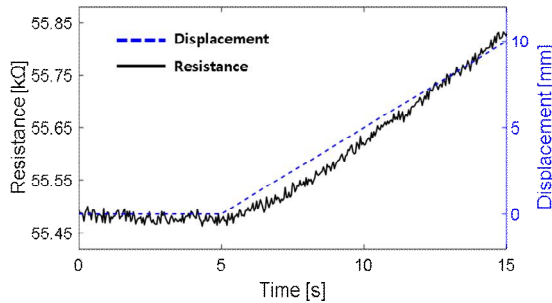
$$R = \rho \frac{L}{A}, \quad \rho = \frac{AR}{L} \dots\dots\dots (1)$$

R : electrical resistance(Ω),

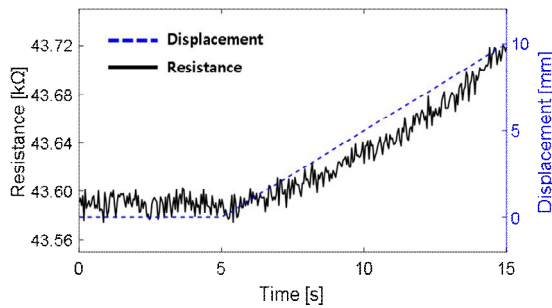
ρ : specific resistance($\Omega \cdot \text{mm}$)

L : specimen length (mm),

A : specimen's cross-section area (mm^2)

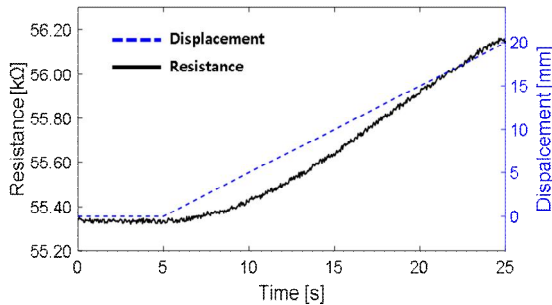


• Straight curve electrode sensor

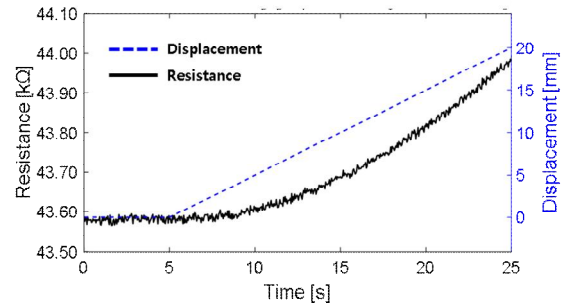


• Hilbert curve electrode sensor

(a) 10mm bending displacement-resistance curve

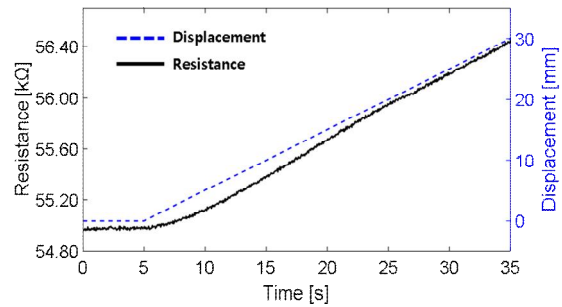


• Straight curve electrode sensor

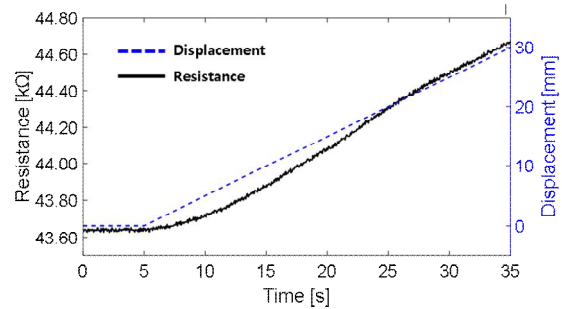


• Hilbert curve electrode sensor

(b) 20mm bending displacement-resistance curve



• Straight curve electrode sensor



• Hilbert curve electrode sensor

(c) 30mm bending displacement-resistance curve

Fig. 7 Strain(blue dashed line)-Resistance(black solid line) curve

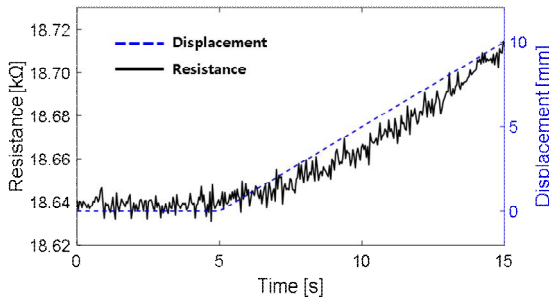
2.2 Comparison of electrical characteristics due to annealing of 3D printing flexible resistance sensor

To analyze the effect of annealing on 3D printing FBS, the change in electrical resistance was measured using the same process of the above experiment

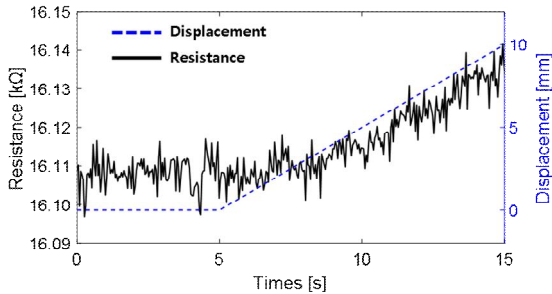
method after annealing the bending sensor. Annealing was conducted at a constant temperature oven at 120°C (crystallization temperature of conductive filament in the printing electrode) for two hours and then oven cooling was performed in the constant temperature oven at room temperature.

Fig. 8 shows the measurement results of the change in electric resistance according to the iterative test of bending and returning-back of 10, 20, and 30 mm in the bending sensor center after annealing of FBS. The figure shows that the bending displacement and electric resistance are proportional over time, and the electric resistance is significantly lower than that before annealing.

The resistance changes (ΔR) of straight and Hilbert curve electrode sensors according to bending displacements of 10, 20, and 30 mm in the printing bending sensor were 0.07, 0.15, and 0.31 k Ω , and 0.03, 0.09, and 0.17 k Ω , respectively, which were all increased in proportion to the bending displacement.

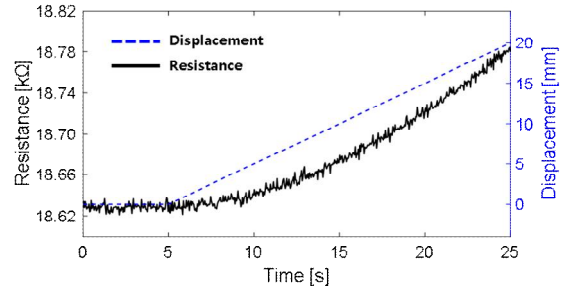


• Straight curve electrode sensor

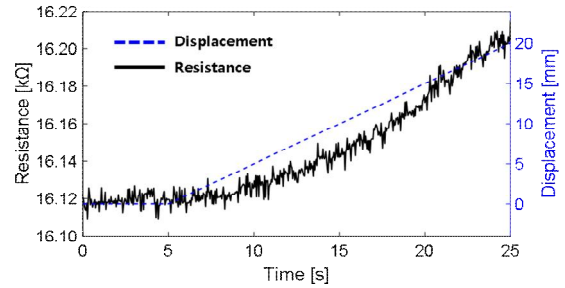


• Hilbert curve electrode sensor

(a) 10mm bending displacement-resistance curve

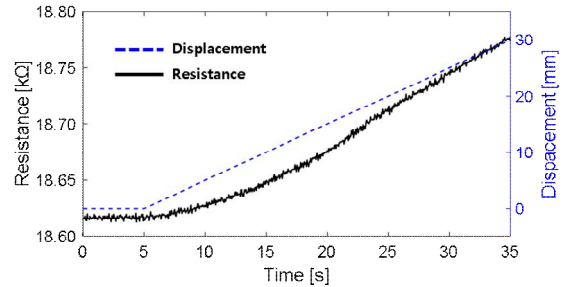


• Straight curve electrode sensor

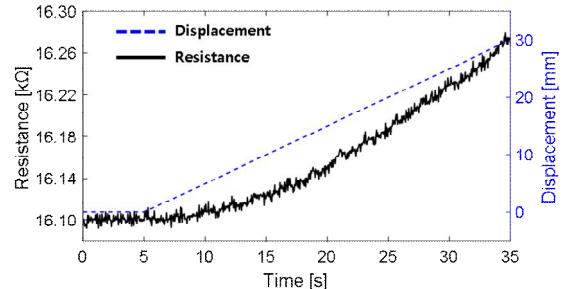


• Hilbert curve electrode sensor

(b) 20mm bending displacement-resistance curve



• Straight curve electrode sensor



• Hilbert curve electrode sensor

(c) 30mm bending displacement-resistance curve

Fig. 8 Strain(blue dashed line)-Resistance(black solid line) curve after annealing

In addition, the resistance change of the straight curve electrode sensor was larger than that of the Hilbert curve electrode sensor, which was the same before annealing. The reason for the lower initial resistance, resistance against maximum displacement, and changes in resistance of bending sensor after annealing compared to those before annealing was the active atom diffusion of printing electrode by annealing, which removed the strain energy stored in the inside due to the dislocation movements. This resulted in the reduction in vacancy and removing the dislocation, which was a unstable defect in terms of energy, which led to the improvement of electrical conductance^[7-8].

3. Review and discussion

Table 1 presents the changes in electric resistance according to bending displacement before and after annealing of the 3D printing FBS. In all displacements, the electric resistance of Hilbert curve electrode sensor was lower than that of the straight curve electrode sensor.

Generally, since the polymer is oriented in the resin flow direction, a difference in shrinkage ratio occurs between the flow and perpendicular directions. This is because the orientation of the straight curve electrode was relatively longer when seeing the laminating direction in the resin flow direction by moving the high-temperature extrusion nozzle during 3D printing, inducing shrinkage of the straight curve electrode in the longitudinal direction larger than that of the Hilbert curve electrode. This results in a tendency to compensate the shrinkage in the direction perpendicular to orientation, which was led to larger electric resistance of the straight curve electrode. In addition, because the continuous travel distance of the printing high-temperature extrusion nozzle of the straight curve electrode was relatively longer, instability of polymer crystal grain due to high-temperature extrusion and room-temperature

Table 1 3D printing flexible sensor resistance

		δ (mm)	R_0 [k Ω]	R_{max} [k Ω]	$\Delta R/R_0$ [%]
Straight curve sensor	No annealing	10	55.48	55.83	0.63
	annealing		18.64	18.71	0.38
Hilbert curve sensor	No annealing		43.59	43.72	0.30
	annealing		16.11	16.14	0.19
Straight curve sensor	No annealing	20	55.34	56.16	1.48
	annealing		18.63	18.78	0.81
Hilbert curve sensor	No annealing		43.57	43.99	0.964
	annealing		16.12	16.21	0.56
Straight curve sensor	No annealing	30	54.98	56.43	2.64
	annealing		18.64	18.95	1.66
Hilbert curve sensor	No annealing		43.64	44.67	2.36
	annealing		16.10	16.27	1.06

δ : Bending displacement, R_0 : Base resistance,

R_{max} : Resistance at the max. bending, ΔR : $R_{max} - R_0$

$\Delta R/R_0$: Resistance change ration

lamination (rapid cooling) and shear flow due to friction and cooling in the inside and high-temperature nozzle wall surface were larger than those of the Hilbert curve electrode. This resulted in relatively larger electric resistance as the residual stress of the straight curve electrode was larger^[7-10].

Fig. 9 shows a graph of resistance change ($\Delta R / R_0$), in which the straight curve electrode sensor has better displacement-sensing capability than that of the Hilbert curve electrode sensor.

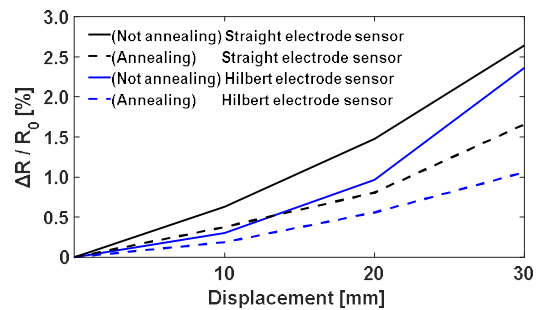


Fig. 9 Displacement-Resistance change ration curve of Straight and Hilbert curve electrode bending sensor

This linearly increasing curve was exhibited because the resistance of the TPU, which was a support, was relatively smaller during the straight curve electrode bending due to the design difference.

4. Conclusions

This study manufactured an FBS using FDM 3D printing and verified its applicability through experiments on changes in electric resistance against bending displacement. In addition, this study found that the electrode stability according to the 3D printing bending sensor design acted as an important variable to sensor sensing capability.

The experimental results showed that the straight curve electrode sensor was better in sensing capability of the 3D printing FBS, while the Hilbert curve electrode sensor was better in electrical conductance. This meant that the measurement range of the FBS could be set differently depending on the electrode shape as a result of the electrode design difference. Thus, a variety of studies should be conducted on various printing electrode designs and electrode stability using annealing and elasticity force of flexible support to improve the performance of 3D printing bending sensors and expand the utilization range. The above results imply that various FBSs with multiple DOFs can be manufactured by a simple 3D printing process without the limitation of size and shape, which will be employed usefully as a major factor in the flexible electric and electronic applied device development using 3D printing.

Acknowledgement

This paper was supported by the funding of the project on the development of biomedical technology (NRF-2017M3A 9E2063256) from the National Research Foundation of Korea in the Ministry of Science and ICT, and FDM-based multi-material 4D printing and structural design made of Vitremer composite material (Grants No. NRF-2019M3D1A2103919).

References

1. Pal, R. K., Farghaly, A. A., Collinson, M. M., Kundu, S. C., Yadavalli, V. K., "Photolithographic Micropatterning of Conducting Polymers on Flexible Silk Matrices," *Advanced Materials*, Vol. 28, No. 7, pp. 107~116, 2015.
2. Ana, M., Gemma G., Rosa, V., and Javier del Campo, F., "Inkjet-printed Electrochemical Sensors," *Current Opinion in Electrochemistry*, Vol 3, No. 1, pp. 29 ~39, 2017.
3. Bariya, M., Shahpar, Z., Park, H., Sun, J., Jung, Y., Gao, W., Nyein, H. Y. Y., Liaw, T. S., Tai, L-C., Ngo, Q. P., Chao, M., Zhao, Y., Hettick, M., Cho, G., Javey, A., "Roll-to-Roll Gravure Printed Electrochemical Sensors for Wearable and Medical Devices" *American Chemical Society*, Vol. 12, No. 7, pp.6978~6987, 2018.
4. Bhat, K. S., Ahmad, R., Yoo, J-Y. Hahn, Y. B., "Nozzle-jet printed flexible field-effect transistor biosensor for high performance glucose detection," *Journal of Colloid and Interface Science*, Vol. 506, pp. 188~196, 2017.
5. Nomura, K-I., Kaji, R., Iwata, S., Otao, S., Imawaka, N., Yoshino, K., Mitsui, R., Sato, J., Takahashi, S., Nakajima, S-I., and Ushijima, H., "A flexible proximity sensor formed by duplex screen/screen-offset printing and its application to non-contact detection of human breathing," *Journal of nature*, Vol. 6, pp. 6~10, 2016.
6. Jackson Jr, W. J., Caldwell, J., R., "Antiplasticization . II. Characteristics of antiplasticizers," *Journal of Applied Polymer*, Vol 11, Issue 2, pp 211~226, 1967.
7. Lee, S. K., Kim, Y. R., Park, J. H., Kim, J. H., "Study on Electrical Characteristics of FDM Conductive 3D Printing According to Annealing Conditions", *Journal of the Korean Society of Manufacturing Process Engineers*, Vol. 17, No. 6, pp. 55~60, 2018.
8. Hashima, K., Nishitsuji, S., Inoue, T., "Structure-properties of super-tough PLA alloy with excellent

- heat resistance,” *Polymer*, Vol. 51, No. 17, pp. 3934-3939, 2010.
9. Postiglione, G., Natale, G., Griffini, G., Levi, M., Turri, S., "Conductive 3D Microstructures by Direct 3D Printing of Polymer/carbon Nanotube Nanocomposites via Liquid deposition modeling,” *Composites Part A*, Vol. 76, pp. 110~114, 2015.
10. Seol, K-S., Shin, B-C., Zhang, S-U., "Fatigue Test of 3D-printed ABS Parts Fabricated by Fused Deposition Modeling,” *Journal of the Korean Society of Manufacturing Process Engineers*, Vol. 17, No. 3, pp. 93~101, 2018.